Biochimica et Biophysica Acta 1857 (2016) 34–45

Contents lists available at ScienceDirect

Biochimica et Biophysica Acta

journal homepage: www.elsevier.com/locate/bbabio

Specific degradation of phosphatidylglycerol is necessary for proper mitochondrial morphology and function

Lucia Pokorná [a], Petra Čermáková [b], Anton Horváth [b], Matthew G. Baile [c], Steven M. Claypool [c], Peter Griač [a], Jan Malínský [d], Mária Balážová [a,*]

[a] Department of Membrane Biochemistry, Institute of Animal Biochemistry and Genetics, Slovak Academy of Sciences, Ivanka pri Dunaji, Slovakia
[b] Department of Biochemistry, Faculty of Natural Sciences, Comenius University, Bratislava, Slovakia
[c] Department of Physiology, School of Medicine, Johns Hopkins University, Baltimore, MD, USA
[d] Microscopy Unit, Institute of Experimental Medicine, Academy of Sciences of the Czech Republic, Prague, Czech Republic

ARTICLE INFO

Article history:
Received 12 June 2015
Received in revised form 22 September 2015
Accepted 15 October 2015
Available online 19 October 2015

Keywords:
Yeast
Phosphatidylglycerol
Mitochondria
Morphology
Respiration

ABSTRACT

In yeast, phosphatidylglycerol (PG) is a minor phospholipid under standard conditions; it can be utilized for cardiolipin (CL) biosynthesis by CL synthase, Crd1p, or alternatively degraded by the phospholipase Pgc1p. The *Saccharomyces cerevisiae* deletion mutants *crd1Δ* and *pgc1Δ* both accumulate PG. Based on analyses of the phospholipid content of *pgc1Δ* and *crd1Δ* yeast, we revealed that in yeast mitochondria, two separate pools of PG are present, which differ in their fatty acid composition and accessibility for Pgc1p-catalyzed degradation. In contrast to CL-deficient *crd1Δ* yeast, the *pgc1Δ* mutant contains normal levels of CL. This makes the *pgc1Δ* strain a suitable model to study the effect of accumulation of PG *per se*. Using fluorescence microscopy, we show that accumulation of PG with normal levels of CL resulted in increased fragmentation of mitochondria, while in the absence of CL, accumulation of PG led to the formation of large mitochondrial sheets. We also show that *pgc1Δ* mitochondria exhibited increased respiration rates due to increased activity of cytochrome *c* oxidase. Taken together, our results indicate that not only a lack of anionic phospholipids, but also excess PG, or unbalanced ratios of anionic phospholipids in mitochondrial membranes, have harmful consequences on mitochondrial morphology and function.

© 2015 Elsevier B.V. All rights reserved.

1. Introduction

Mitochondrial membranes represent a highly specialized functional unit comprised of two different lipid bilayers. The composition of the inner mitochondrial membrane (IMM) is quite unusual, exhibiting a low phospholipid:protein (mg/mg) ratio of 0.15, whereas in the outer mitochondrial membrane (OMM), this ratio is up to 0.91 [1,2,3]. The IMM also contains two specific anionic phospholipids: phosphatidylglycerol (PG) and cardiolipin (CL).

CL, a unique dimeric phospholipid exclusive to mitochondrial membranes, is synthesized in yeasts in a reaction of PG with cytidine diphosphate-diacylglycerol (CDP-DAG), catalyzed by the CL synthase, Crd1p [4,5,6]. Under standard conditions, PG in yeasts is a minor phospholipid that is mainly used for CL biosynthesis. Alternatively, PG can be degraded to DAG and glycerol-3-phosphate (G3P) by the PG specific phospholipase Pgc1p [7]. Accordingly, yeast lacking either *CRD1* or *PGC1* accumulate PG. In the *crd1Δ* strain, accumulation of PG is accompanied by the absence of CL [4,5,6,8,9]; in *pgc1Δ* cells, PG accumulates but does not cause significant changes in other phospholipids, including CL [7]. Thus, the *pgc1Δ* strain provides an excellent model in which to study the effects of changes in PG levels independent of changes in CL or other phospholipids.

Diverse biological functions of these two anionic phospholipids have been described. All proteins of the oxidative phosphorylation (OXPHOS) system have high affinity binding sites for CL. CL thus represents a major phospholipid necessary for the proper function of respiratory complexes and for the stability of OXPHOS supercomplexes [10,11]. CL also acts as a proton trap and provides a source of charge during OXPHOS [12]. Furthermore, CL is required for protein import [9], formation of cristae morphology [13,14], mitochondrial fusion [15,16], cellular iron homeostasis [17] and apoptosis [18,19], reviewed in [20]. PG, aside from its essential role in CL biosynthesis, also fulfills various functions in specific membranes of some eukaryotic organisms. For example, PG is the sole phospholipid of thylakoid membranes in eukaryotic oxygenic

Abbreviations: CCCP, carbonyl cyanide m-chlorophenyl hydrazine; CL, cardiolipin; DAG, diacylglycerol; ER, endoplasmic reticulum; ETS, electron transport system; G3P, glycerol-3-phosphate; I, inositol; IMM, inner mitochondrial membrane; OMM, outer mitochondrial membrane; OXPHOS, oxidative phosphorylation; PG, phosphatidylglycerol; PGP, phosphatidylglycerolphosphate; PI, phosphatidylinositol; RCI, respiration control index; SMD, glucose synthetic minimal medium; SMDGE, glucose, glycerol and ethanol synthetic minimal medium; WT, wild type.

* Corresponding author at: Institute of Animal Biochemistry and Genetics, Slovak Academy of Sciences, Moyzesova 61, 900 28, Ivanka pri Dunaji, Slovakia.
E-mail address: Maria.Balazova@savba.sk (M. Balážová).

http://dx.doi.org/10.1016/j.bbabio.2015.10.004
0005-2728/© 2015 Elsevier B.V. All rights reserved.

photosynthetic organisms [21,22] and it is an important component of pulmonary surfactant, an essential fluid produced by alveolar type II cells that covers the entire surface of the lung [23]. In yeast cells, PG is a low abundance phospholipid, even under the conditions of aerobic growth [6]. Therefore, PG is mainly considered to be a metabolic precursor of CL in yeast.

The absence of CL in mitochondrial membranes is associated with pleiotropic defects. The *crd1Δ* yeast strain displays growth defects and decreased viability on both fermentable and nonfermentable carbon sources at elevated temperatures, decreased mitochondrial membrane potential, and decreased respiratory rates [8,9,24]. Respiratory chain supercomplexes are destabilized in *crd1Δ* cells [14,25,26] and the lack of CL leads to mitochondrial DNA instability [8,9,27].

The absence of both PG and CL, which occurs upon deletion of *PGS1*/*PEL1*, the gene encoding phosphatidylglycerolphosphate (PGP) synthase (Pgs1p), causes even more severe phenotypes: its growth is strictly dependent on the presence of a fermentable carbon source in the media and its temperature sensitivity is higher compared to *crd1Δ* yeast [28,29,30,31,32,33]. This remarkable difference between the *crd1Δ* and *pgs1Δ* strains, which both lack CL but contain different amounts of PG, indicates that either PG can partially substitute for some essential functions of CL or some functions ascribed to CL could in fact be mediated by PG [9,34]. This interpretation is supported by other observations. For example, the defective translation of mRNA coding for Cox4p, an essential subunit of cytochrome *c* oxidase, detected in *pgs1Δ* cells is directly caused by the lack of PG and CL in mitochondrial membranes. In the absence of these lipids, binding of a protein factor(s) specifically to 5′ *cis* element of *COX4* mRNA is observed, which inhibits translation and lowers the Cox4p levels in *pgs1Δ* cells [35]. In contrast, the *crd1Δ* mutant, which contains PG, has normal Cox4p protein levels [14]. Similarly, activation of Isc1p, the inositol sphingolipid phospholipase C, after the diauxic shift is dependent on *PGS1* but not on *CRD1* [36]. These results suggest that PG could play roles beyond just being a biochemical precursor of CL or a structural part of mitochondrial membranes, and instead is itself an important player in various cell functions.

Most defects in *crd1Δ* cells are attributed to the absence of CL. Nevertheless, these cells also accumulate PG. In this study, we asked whether the accumulation of PG alone could generate some of the defects observed in *crd1Δ* yeast. We used the *pgc1Δ* mutant, which contains normal levels of CL but elevated PG, to characterize the specific effects of PG accumulation on mitochondrial respiration and morphology. Comparison of *pgc1Δ* and CL-deficient (*crd1Δ* and *pgc1Δcrd1Δ*) yeast allowed us to distinguish the effects of the absence of CL from the accumulation of PG. Based on our data, we report that PG accumulation induces defects in mitochondrial morphology. Further, accumulation of PG caused respiratory defects, mainly increased respiration rates and uncoupling, associated with activation of cytochrome *c* oxidase.

2. Materials and methods

2.1. Yeast strains and growth conditions

All yeast strains used in this study are listed in Table 1. Cultures were maintained on complex YPD media (2% yeast extract, 1% peptone, 2% glucose). For experiments, yeast were grown aerobically at 28 °C in defined synthetic medium prepared as described previously [37] with various carbon sources: SMD (2% glucose) or SMDGE (0.2% glucose, 3% glycerol, 1% ethanol). Synthetic medium was either supplemented with 75 μM inositol (I+) or lacked inositol (I-). Transformants were selected on synthetic medium without uracil.

2.2. RNA isolation and RT-qPCR analysis

The yeast cells were grown in SMD medium with or without inositol to the indicated growth phase. Total RNA was isolated from $3x10^8$ cells. Briefly, cells were broken by vortexing with 150 μl of glass beads in 100 μl of 10 mM TrisHCl, pH 8.0; 0.1 mM EDTA pH 8.0 for 3 × 45 s with 1 min cooling on ice in between. RNA was purified using the GeneJet RNA kit (ThermoScientific). RNA was eluted with 100 μl of water. 10–20 μg of isolated RNA was treated with DNase I to eliminate DNA contamination. DNase was removed using the RapidOut DNA removal kit (ThermoScientific). Purified RNA was reverse transcribed to cDNA using the RevertAid Premium First Strand cDNA Synthesis Kit (ThermoScientific). Final cDNA was diluted 10 times, and a 5 μl aliquot was used for qPCR analysis with the following primers: *PGC1* (sense, 5′-AGCGATGGTATGGTGGTGG-3′; antisense, 5′-GGAACCATCCTCTTTG CAGC-3′), *ACT1* (sense, 5′-ACCGCTGCTCAATCTTCTTC-3′; antisense, 5′-GGTCAATACCGGCAGATTCC-3′), *IPP1* (sense, 5′-ATGAAGGTGAGACCGA TTGG-3′; antisense, 5′-CTGGCTTACCATCTGGGATT-3′), and FastStart Essential DNA Green master (Roche) according to the manufacturer's instructions. *PGC1*, *ACT1* and *IPP1* transcripts were analyzed on the LightCycler 96 (Roche). PCR products were confirmed by melting curve analysis. Standard curves were generated from PCR amplification of template dilutions. Final data were normalized to *ACT1* and *IPP1* mRNA levels, and mRNA levels in wild type (WT) cells were set to 1.

2.3. Analysis of fatty acids

Extraction of phospholipids was performed by addition of 4.5 ml of chloroform–methanol–HCl (60:30:0.26) to mitochondrial extracts corresponding to 1 mg of proteins, followed by 30 min incubation at RT. Subsequently, 4.5 ml of 0.1 M $MgCl_2$ was added and following a brief vortex, incubated for another 30 min at RT. Phases were separated by centrifugation. The organic phase was dried under a stream of nitrogen. Phospholipids were separated by one-dimensional thin layer chromatography on silica plates using chloroform–methanol–acetic acid (65:25:8) [38].

Table 1
Yeast strains. All strains were in BY4741 or BY4742 background.

Strain	Genotyp	Source
pgc1Δ	*MATα his3, leu2, ura3, lys2, pgc1::KanMX*	Research Genetics
pgc1Δ + EV	*MATα his3, leu2, ura3, lys2, pgc 1::KanMX*, YEplac195 (URA3)	[7]
pgc1Δ + *PGC1*	*MATα his3, leu2, ura3, lys2, pgc 1::KanMX*, YEplac195-*PGC1*	[7]
WT	*MATa his3, leu2, met15, ura3, lys2*	Research Genetics
WT + EV	*MATa his3, leu2, met15, ura3, lys2*, YEplac195 (URA3)	[7]
WT + *PGC1*	*MATa his3, leu2, met15, ura3, lys2*, YEplac195-*PGC1*	[7]
crd1Δ	*MATa his3, leu2, met15, ura3, crd1::KanMX*	Research Genetics
crd1Δ + EV	*MATa his3, leu2, met15, ura3, crd1::KanMX*, YEplac195 (URA3)	This study
crd1Δ + *PGC1*	*MATa his3, leu2, met15, ura,3 crd1::KanMX*, YEplac195-*PGC1*	This study
pgc1Δcrd1Δ	*MATa leu2, ura3, met15, crd1::KanMX, pgc1::HIS3*	[7]
pgc1Δcrd1Δ + EV	*MATa leu2, ura3, met15, crd1::KanMX, pgc1::HIS3*, YEplac195 (URA3)	This study
pgc1Δcrd1Δ + *PGC1*	*MATa leu2, ura3, met15, crd1::KanMX, pgc1::HIS3*, YEplac195-*PGC1*	This study
pgc1Δcrd1Δ + *PDA1-GFP*	*MATa leu2, ura3, met15, crd1::KanMX, pgc1::HIS3*, pUG35-*PDA1-GFP* (URA3)	This study
pgc1Δcrd1Δ + *ss-GFP-HDEL*	*MATa leu2, ura3, met15, crd1::KanMX, pgc1::HIS3*, Ylp211-*TRP1-TKC-GFP-HDEL* (URA3)	This study

The resolved spot of PG was scraped from the plate and extracted by 1 ml of hexane.

Fatty acids from PG were converted to their methyl esters by the method of Christoperson and Glass [39]. Analysis was performed by the application of 1 μl aliquots to a gas chromatography apparatus (GC2010Plus, Shimadzu, Japan) equipped with BPX70 capillary column (30 m × 0.25 mm × 0.25 μm, SGE Analytical Science, Australia) under temperature programming (160–234 °C at 4.5 °C/min increments). Individual fatty acid methylesters were identified by comparison with authentic standards of C4 — C24 fatty acid methylesters mixture (Supelco, USA).

2.4. Fluorescence microscopy

Living yeast cells grown in SMDGE medium were concentrated by brief centrifugation, immobilized on a 0.17 mm coverglass by a thin film of 1% agarose diluted in 50 mM phosphate buffer pH 6.3 and observed using LSM510-META confocal microscope (Zeiss) with a 100× PlanApochromat oil-immersion objective (NA = 1.4). Fluorescence signals of GFP and Mitotracker Red CMX-Ros (excited by 488 nm line of Ar laser, and 561 nm line of solid state laser) were detected using bandpass 505–550, and 575–615 nm emission filters, respectively. The length of mitochondria was analyzed with ImageJ software (ImageJ, U. S. National Institutes of Health, Maryland, USA).

2.5. Measurement of mitochondrial respiration and OXPHOS

Yeast cells were grown in SMDGE medium with or without inositol for 24 h. Intact mitochondria were isolated as described previously [7] with a modified homogenization buffer: 0.6 M mannitol, 20 mM HEPES/KOH pH 7.1, 1 mM EGTA, 0.2% (*w*/*v*) fatty acid free bovine serum albumin. The final mitochondrial pellet was suspended in the homogenization buffer at ~10 mg/ml of protein. The reaction buffer used for mitochondrial respiration and OXPHOS studies was 0.6 M mannitol, 20 mM Hepes/KOH pH 7.1, 2 mM $MgCl_2$, 1 mM EGTA, and 0.1% (*w*/*v*) fatty acid free bovine serum albumin. Respiration rates were measured with a Clark-type oxygen electrode (Hansatech). The final concentration of mitochondrial proteins in the reaction mixture was 150 μg/ml, 1 ml of the reaction mixture was used. NADH (0.5 mM) was used as a respiratory substrate. Phosphorylation was estimated from ADP-stimulated respiration using total oxygen consumption. The concentration of ADP in each reaction was 0.2 mM. Mitochondria were uncoupled by the addition of 15 μM carbonyl cyanide m-chlorophenyl hydrazine (CCCP).

2.6. Enzymatic assays

The mitochondrial lysate was prepared by suspending mitochondria in 0.5 M aminocaproic acid and dodecyl maltoside to the final concentration of 2% (*w*/*v*) and lysis was performed for 60 min on ice. Lysate was centrifuged at 15,000 *g* for 10 min at 4 °C. Supernatant was used in further analyses. Activity of cytochrome *c* reductase was measured in 1 ml of QCR buffer (40 mM Na-phosphate buffer pH 7.4, 0.5 mM EDTA pH 8.5, 20 mM sodium malonate, 50 μM cytochrome *c*, and 0.005% (*w*/*v*) dodecyl maltoside). Simultaneously, 2 μl of the mitochondrial lysate and 2 μl of 2,3-dimethoxy-5-methyl-6-decyl-1,4-benzoquinol were added and the reaction was monitored at 550 nm for 1 min.

Activity of cytochrome *c* oxidase was measured in 1 ml of COX buffer (40 mM Na-phosphate buffer pH 7.4, 0.5 mM EDTA pH 8.5, 20 μM cytochrome *c*, 30 μM ascorbic acid, 0.005% (*w*/*v*) dodecyl maltoside; solution was allowed to stand overnight to oxidize surplus of ascorbic acid). 2–5 μl of the mitochondrial lysate were added to the buffer and the reaction was monitored at 550 nm for 5 min.

ATP-hydrolase activity was measured in 1 ml of TC buffer (200 mM KCl, 10 mM Tris/HCl pH 8.2, 2 mM $MgCl_2$) using 1 mg of the mitochondrial proteins. The reaction was started at 37 °C by the addition of ATP to a final concentration of 5 mM. After 5 and 10 min, respectively, 95 μl of the mixture was transferred into a new 1.5 ml tubes containing 5 μl of 3 M trichloroacetic acid. The mixture was incubated on ice for 30 min and then centrifuged at 16,000 *g* for 10 min at 4 °C. One ml of the Sumner reagent (8.8% (*w*/*v*) $FeSO_4$ x$7H_2O$, 375 mM H_2SO_4, 6.6% (*w*/*v*) $(NH_4)_6Mo_7O_{24}$ x$4H_2O$) was mixed with 90 μl of the mitochondrial supernatant and incubated at room temperature for 15 min. The absorbance was measured at 610 nm.

2.7. In-gel activity staining

For activity staining, mitochondria were suspended in 0.5 M aminocaproic acid and digitonin was added for a 3:1 ratio of digitonin/mitochondrial proteins (*w*/*w*). The lysis mixture was incubated 60 min on ice. The lysate was centrifuged for 10 min at 15,000 *g* at 4 °C and the protein concentration was determined by the Bradford assay [40]. 50 μg of proteins from mitochondrial lysate was mixed with 1.5 μl CB solution (0.5 M aminocaproic acid, 5% (*w*/*v*) Coomassie Brilliant Blue G-250), incubated for 10 min on ice and separated on 3–9% gradient blue native gel with a power limit of 1.5 W at 4 °C as described [41]. After the run, the gel was stained in the reaction buffer. ATPase activity was visualized using 35 mM Tris containing 270 mM glycine, 14 mM $MgSO_4$, 0.2% (*w*/*v*) $Pb(NO_3)_2$ and 8 mM ATP. Staining took place overnight at RT.

2.8. Western blot analysis

Proteins obtained upon mitochondrial lysis were separated either on 3–9% native or 12% denaturing polyacrylamide gels and blotted onto a nitrocellulose membrane. The membrane was blocked using 5% milk in TBS buffer (50 mM Tris/HCl pH 8.0, 150 mM NaCl, 0.05% (*v*/*v*) Tween 20) overnight. Then, the membrane was immunostained using the following antibodies: Complex III, rabbit anti-Rip1p MGB72.T (dilution 1:500); Complex IV, mouse monoclonal anti-Cox2p 4B12 (dilution 1:500) and rabbit anti-Cox4p (1:1000). Visualization of secondary anti-mouse (Sigma) or anti-rabbit (Sigma) antibodies was done using ECL+ kit (Amersham) or NCBI/BHT kit (Sigma).

2.9. Miscellaneous

Preparation of mitochondria, steady-state phospholipid analysis, and measurements of Pgc1p and PGP synthase activity were performed as described previously [7]. Statistical comparisons were carried out by one-way analysis of variance using SigmaPlot 11 software (Systat software, San Jose, CA). All graphs show the mean ± SEM.

3. Results

3.1. CL synthase, Crd1p, and phospholipase C, Pgc1p, utilize distinct pools of PG

We compared PG and CL levels in strains lacking *PGC1* and/or *CRD1* grown under respiratory conditions in synthetic minimal media containing glycerol and ethanol as carbon source (SMDGE), with (I+) or without (I-) inositol (Fig. 1). Inositol is a soluble precursor of phosphatidylinositol (PI) and a known major regulator of phospholipid biosynthesis [42,43]. The CL biosynthetic pathway has been shown to be repressed by exogenous inositol at the rate-limiting step of the pathway, conversion of CDP-DAG to PGP by the PGP synthase, Pgs1p [28,29].

All tested mutant strains, *pgc1Δ*, *crd1Δ*, and *pgc1Δcrd1Δ*, contained significantly increased levels of PG compared to the WT. The additive effect of the double deletion mutant, *pgc1Δcrd1Δ*, indicates that processes of PG utilization, either for biosynthesis of CL by Crd1p or for degradation to DAG and G3P by Pgc1p, are mutually independent. The effect of exogenous inositol was much more pronounced in strains lacking *PGC1*. The relative amounts of PG in these strains were much higher when cells were grown in SMDGE I− medium compared to SMDGE I+. In strains

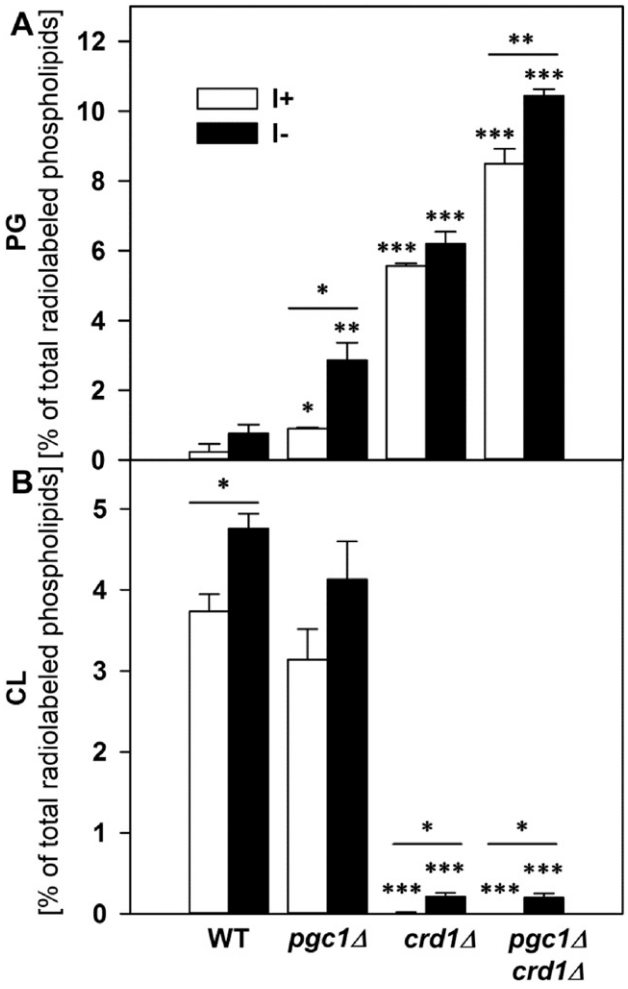

Fig. 1. Pgc1p buffers PG levels in yeast. *S. cerevisiae* cells were grown in SMDGE I− or I+ medium in the presence of [^{32}P] orthophosphoric acid for five to six generations. Steady-state phospholipid analysis showing: A, PG as a percentage of [^{32}P] orthophosphoric acid labeled cellular phospholipids and B, CL as a percentage of [^{32}P] orthophosphoric acid labeled cellular phospholipids. Data represent mean values of three experiments ± SEM. Statistically significant differences between mutant strains and WT and between I− and I+ media are marked.*, $p < 0.05$; **, $p < 0.01$; ***, $p < 0.001$.

containing *PGC1*, the effect of exogenous inositol on PG was at the border of statistical significance (Fig. 1A). These results indicate that the PG specific phospholipase C, Pgc1p, is able to partially alleviate the elevation of PG levels, especially in cells grown in media without inositol. Importantly, accumulation of PG in *pgc1Δ* cells was not accompanied by significant changes of CL levels (Fig. 1B). The relative changes of PG fraction in cellular phospholipid content were correlated with the changes of absolute amounts of PG detected in mitochondria isolated from the analyzed strains (Supplementary Fig. S1).

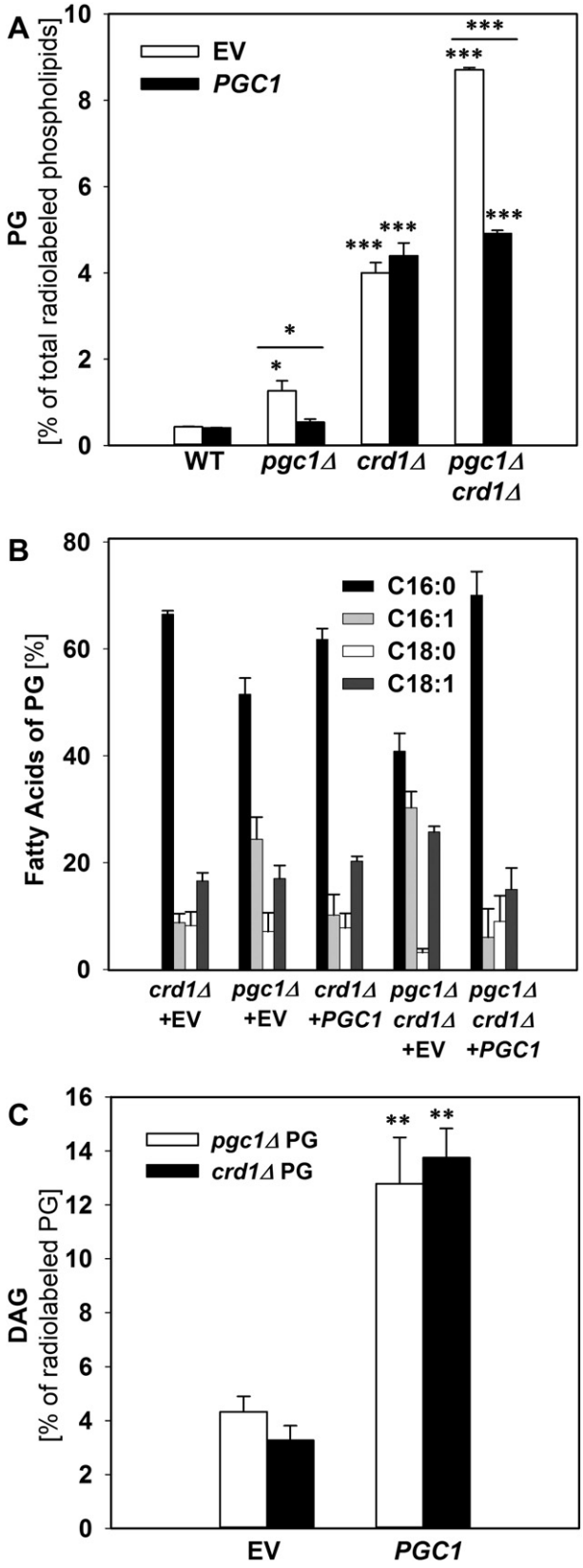

Fig. 2. Deletion of *PGC1* and *CRD1* induces accumulation of PG, which differ in fatty acid composition and accessibility to degradation by Pgc1p. A, Steady-state analysis of total cellular phospholipids. Yeast cells were grown in SMDGE I− URA− medium with [^{32}P] orthophosphoric acid for five to six generations. PG is shown as a percentage of [^{32}P] orthophosphoric acid incorporated into cellular phospholipids. Data represent mean values of three independent experiments ± SEM. Statistically significant differences between mutant strains and WT and between I− and I+ media are marked. *$p < 0.05$; **, $p < 0.01$; ***, $p < 0.001$. B, Gas chromatography analysis of PG fatty acids. Yeast cells were grown in SMD I− URA− media. Relative amounts of individual fatty acids derived from PG extracted from crude mitochondrial fractions are shown. Data represent mean values from two independent experiments ± SEM. C, *In vitro* analysis of Pgc1p activity. Conversion of [^{14}C] PG originated from either *pgc1Δ* or *crd1Δ* cells to DAG is shown. [^{14}C] PG was isolated from either *pgc1Δ* or *crd1Δ* cells that were grown in SMD I− in the presence of [^{14}C] acetate for six generations. Description of the *in vitro* Pgc1p degradation assay could be found in [7]. Data represent mean values of three independent experiments ± SEM. Statistically significant differences between *pgc1Δ* with EV and *PGC1* are marked. **, $p < 0.01$. EV — multicopy empty vector, *PGC1* — multicopy vector containing *PGC1* controlled by its own promotor.

Next, we measured the relative amounts of PG in all studied mutant strains, *pgc1Δ*, *crd1Δ*, and *pgc1Δcrd1Δ*, when *PGC1* is overexpressed (Fig. 2A). Overexpression of *PGC1* from a multicopy plasmid under its own promoter was verified by quantification of *PGC1* mRNA levels and *in vitro* analysis of Pgc1p degradation activity in all strains (data not shown). In *pgc1Δ* cells overexpressing *PGC1* we detected WT levels of PG. In contrast, no decrease in PG was observed in the *crd1Δ* mutant upon *PGC1* overexpression. In the double deletion mutant, *pgc1Δcrd1Δ*, *PGC1* overexpression decreased the relative amounts of PG to the PG levels of the *crd1Δ* strain. These observations indicated that Pgc1p was not capable of degrading the PG pool generated by *CRD1* deletion.

Indeed, fatty acyl chain analysis revealed that PG isolated from the *pgc1Δ* and *crd1Δ* cells significantly differ in their fatty acid composition. Specifically, we found an approximately three-fold increased palmitoleic acid (C16:1) in PG isolated from the *pgc1Δ* cells compared to *crd1Δ*. This increase was fully at the expense of palmitate (C16:0) (Fig. 2B). High relative abundance of C16:0 PG acyl chains detected in *crd1Δ* cells is in a good agreement with the previously published data reporting elevated level of PG in *crd1Δ* cells compared to WT, but with a predominant fraction of C16:0 in both these strains [34]. It is noteworthy that comparison of results obtained in SMDGE and SMD media revealed that the PG fatty acid composition is independent on the carbon source (data not shown). Significantly slower growth rates detected in strains grown in SMDGE URA− I− made problematic to collect enough PG for reasonably accurate gas chromatography analysis under these conditions, however. Therefore, data from strains grown in SMD URA− I− are presented in Fig. 2B.

Analyses of Pgc1p activity using [^{14}C] PG isolated from either *pgc1Δ* or *crd1Δ* strains as a substrate (Fig. 2C) indicated that upon overexpression of *PGC1* in *pgc1Δ* strain, mitochondria exhibited *in vitro* increased Pgc1p activity irrespectively of the origin of PG used as a substrate. Taken together, our results indicate that two separate pools of PG coexist in mitochondria. These two pools differ in their fatty acid composition and accessibility to Pgc1p-catalyzed degradation, but not their ability to be degraded by Pgc1p *per se*.

3.2. Accumulation of PG in the pgc1Δ strain results from increased Pgs1p activity in I− media that is not compensated by Pgc1p activity

Regulation of phospholipid metabolism is a complex process which responds to various intracellular and environmental signals. A substantial part of this regulation in yeast involves inositol, a soluble precursor of PI biosynthesis [43]. Our results showed that accumulation of PG in the *pgc1Δ* strain was much higher in I− medium compared to I+ medium (Fig. 1). Therefore, we asked the question: what was the role of inositol in this enhanced PG accumulation?

First, we compared levels of the *PGC1* transcript in cells grown in the presence and in the absence of exogenous inositol in logarithmic phase, during the diauxic shift and in post-diauxic phase cultures. After the diauxic shift, the amount of *PGC1* mRNA was approximately two-fold higher compared to the logarithmic phase (Fig. 3A). This result is in line with previous transcriptional studies of the genes involved in CL biosynthesis, namely *PGS1* [44,45] and *CRD1* [46], which showed increased expression of these genes after diauxic shift. Independent from the actual expression level, however, the amount of *PGC1* mRNA remained insensitive to the presence of inositol in media (Fig. 3A). We also tested the effect of inositol on Pgc1p *in vitro* activity. No changes in Pgc1p activity were detected, irrespective of whether inositol was added to the growth medium or directly to the *in vitro* enzymatic assay reaction (data not shown).

Next, we tested whether the activity of the PGP synthase, Pgs1p, is regulated by inositol in *pgc1Δ* strains in a similar way as previously described for yeast with wild type *PGC1* gene [45,47]. *In vitro* Pgs1p activity was several-fold higher in I− medium compared to I+ medium in all tested strains, independent of Pgc1p expression (Fig. 3B). Based on these data we conclude that increased accumulation of PG in the *pgc1Δ* strains in the absence of inositol is the result of increased PGP synthesis that is not compensated by regulated removal of excess PG by Pgc1p.

3.3. Absence of Pgc1p induces fragmentation of mitochondrial network

The mitochondrial network undergoes a continuous rearrangement through dynamic fusion and fission events. Several mechanisms involving lipids in this process have been proposed, including CL being essential for fusion of the IMM [15,16]. However, normal mitochondrial morphology was reported in *crd1Δ* yeast when grown in complex (YPD) or synthetic medium with 2% glucose [15,48]. Using Mitotracker stain, we checked the mitochondrial morphology in the strains lacking *CRD1*, *crd1Δ* and *pgc1Δcrd1Δ*, grown in SMDGE, which revealed an increased occurrence of mitochondria coalesced into large, flat sheets resembling the morphology of the cisternae of endoplasmic reticulum (ER) (Fig. 4A,B). The fraction of cells containing Mitotracker-positive

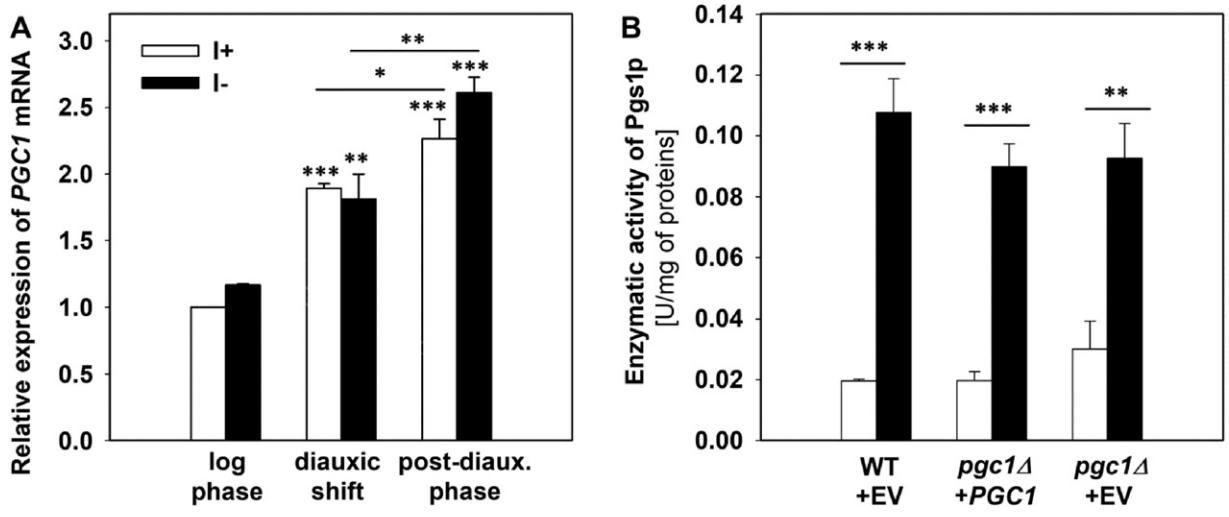

Fig. 3. Expression of *PGC1* is independent of inositol. Enzymatic activity of Pgs1p is increased in I - medium. A, Analysis of *PGC1* transcription. *PGC1* mRNA abundance was analyzed by qRT-PCR following growth of WT cells in SMD I+ or I− media to indicated growth phase. The results were normalized to *ACT1* and *IPP1* mRNA, the mRNA levels in WT I+ cells in log phase of growth were set to 1. Data represent mean values of four independent experiments ± SEM. Statistically significant differences between different phases of growth are marked. *, $p < 0.05$; **, $p < 0.01$; ***, $p < 0.001$. B, *In vitro* enzymatic activity of Pgs1p. Yeast cells were grown in SMD I+ or I− media. PGP synthase activity was determined in mitochondrial fractions. A unit of enzymatic activity is defined as the amount of enzyme that catalyzes the formation of 1 nmol of product/min under the assay conditions described in [7]. Data represent mean values from three independent experiments ± SEM. Statistically significant differences between I− and I+ media are marked. **, $p < 0.01$; ***, $p < 0.001$.

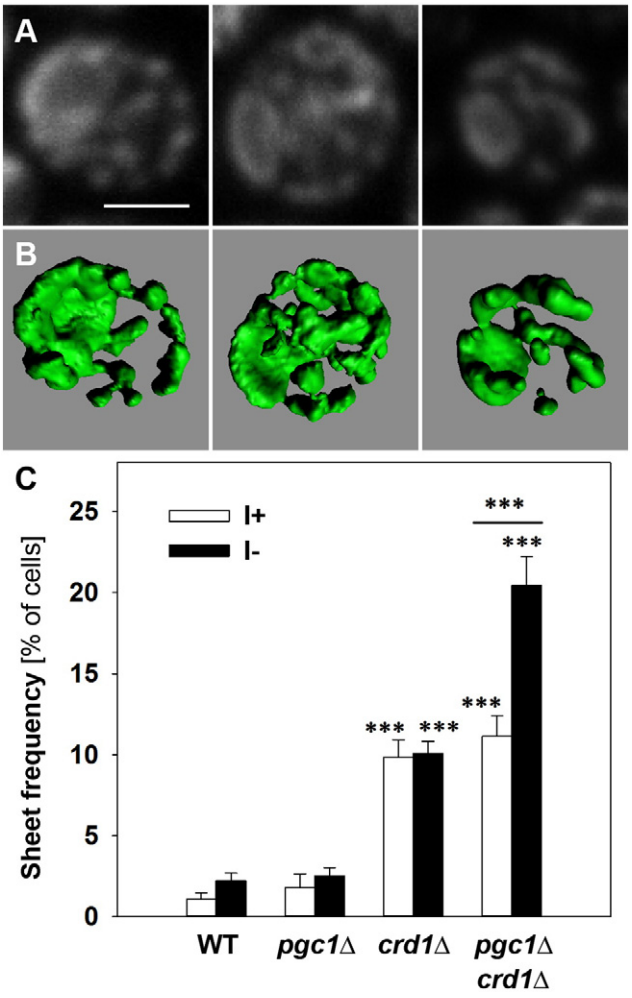

Fig. 4. CL-deficient mutants exhibit flat Mitotracker-stained sheets. Abnormal mitochondria were visualized by Mitotracker Red CMX-Ros staining in cells grown in SMDGE medium for 24 h. A, Three examples of *pgc1Δcrd1Δ* cells containing Mitotracker-stained large flat sheets are presented as mean projections of five consecutive confocal sections from the cell cortex with axial spacing of 370 nm. Flat sheets detected in other analyzed strains including WT were morphologically identical at the resolution of fluorescence microscopy. B, isosurface projections of full 3D stacks, encompassing the whole cell. Bar: 2 μm. C, Statistical evaluation of sheet occurrence in the analyzed strains. Fraction of cells showing this morphological feature was determined in WT, *pgc1Δ*, *crd1Δ* and *pgc1Δcrd1Δ* strain cultures grown in SMDGE I+ or I-media. Data represent mean values of three independent experiments ± SEM. At least 300 cells were evaluated in each experiment. Statistically significant differences between mutant strains and WT and between I− and I+ media are marked. ***, $p < 0.001$.

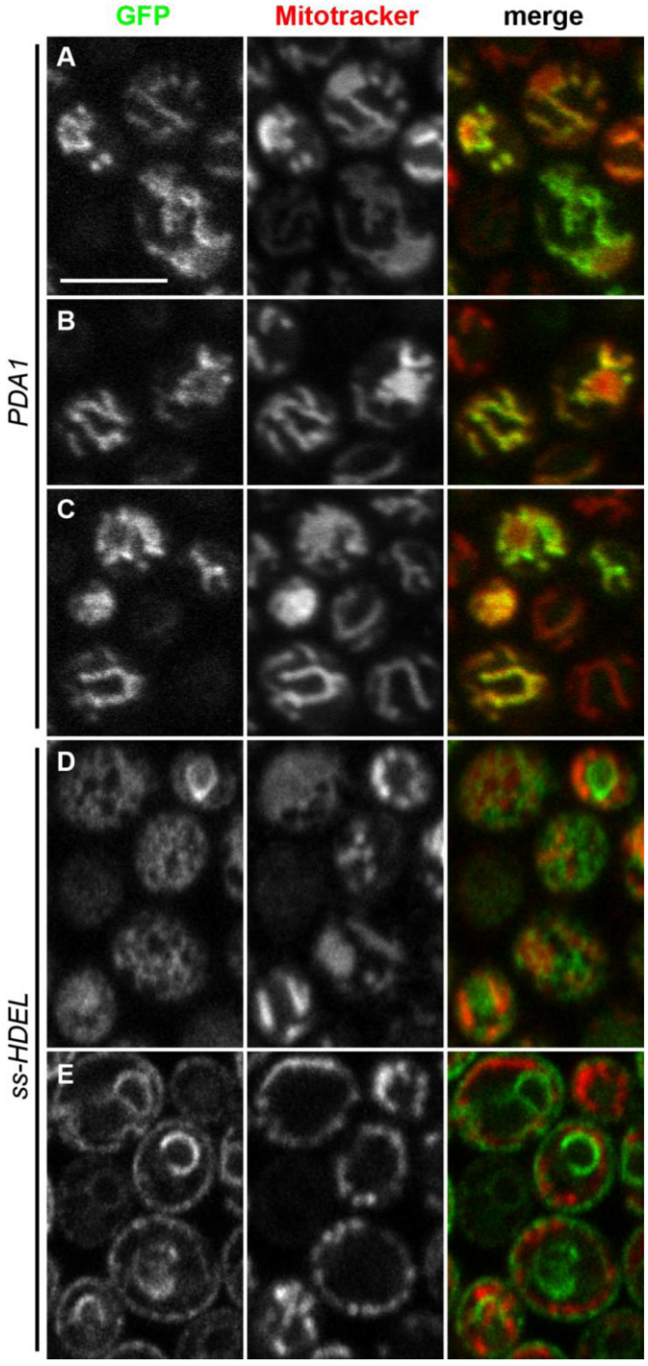

Fig. 5. Flat Mitotracker-stained sheets observed in CL-deficient cells correspond to morphologically abnormal mitochondria. A-C, *pgc1Δcrd1Δ* cells expressing the mitochondrial marker *PDA1-GFP* or D-E, ER marker *ss-GFP-HDEL* were grown in SMDGE I− medium for 24 h, stained with Mitotracker Red CMX-Ros and observed. Mean projections of five consecutive confocal sections from the cell cortex with axial spacing of 370 nm (A-D), and a single transversal confocal section (E) are presented. Bar: 5 μm.

sheets was further increased in the *pgc1Δcrd1Δ* double mutant cultivated in the medium without inositol. *PGC1* deletion alone had no detectable effect in this respect, however (Fig. 4C). The mitochondrial origin of these structures was confirmed by co-localization of the Mitotracker-positive sheets with fluorescently tagged Pda1p, the E1 alpha subunit of the pyruvate dehydrogenase complex that concentrates in spots within the mitochondrial matrix [49,50]. Interestingly, in contrast to the tubular mitochondria, where Pda1-GFP signal covered most of the Mitotracker-stained volume at the resolution of fluorescence microscopy, Pda1-GFP spots overlapping with Mitotracker-stained sheets were confined exclusively to the border of these sheets (Fig. 5A-C). Clear separation of the mitochondrial sheets from the distribution of *ss*-GFP-HDEL, containing a signal sequence for ER localization and the ER retention signal His-Asp-Glu-Leu (HDEL), excluded any overlap of these structures with the ER network (Fig. 5D,E).

To assess the degree of fragmentation of the mitochondrial network in the studied mutant strains, the lengths of individual mitochondria were measured in cells grown in the presence or absence of inositol (Fig. 6). In all analyzed strains, widely dispersed distributions of mitochondrial lengths were detected. Compared to WT, the mutant distributions were shifted towards shorter mitochondria (Fig. 6C). This tendency was most pronounced in *pgc1Δ* cells grown in the absence of inositol, in which we found 71% of mitochondria shorter than 1 μm, compared to 48% in the wild type cells grown in SMDGE I-, and 58% in the *pgc1Δ* cells grown in SMDGE I+. Notably, apart from the *pgc1Δ* strain, the fragmentation of the mitochondrial network was not sensitive to the presence/absence of inositol in the growth medium (Fig. 6C). These results indicated that PG levels significantly contribute

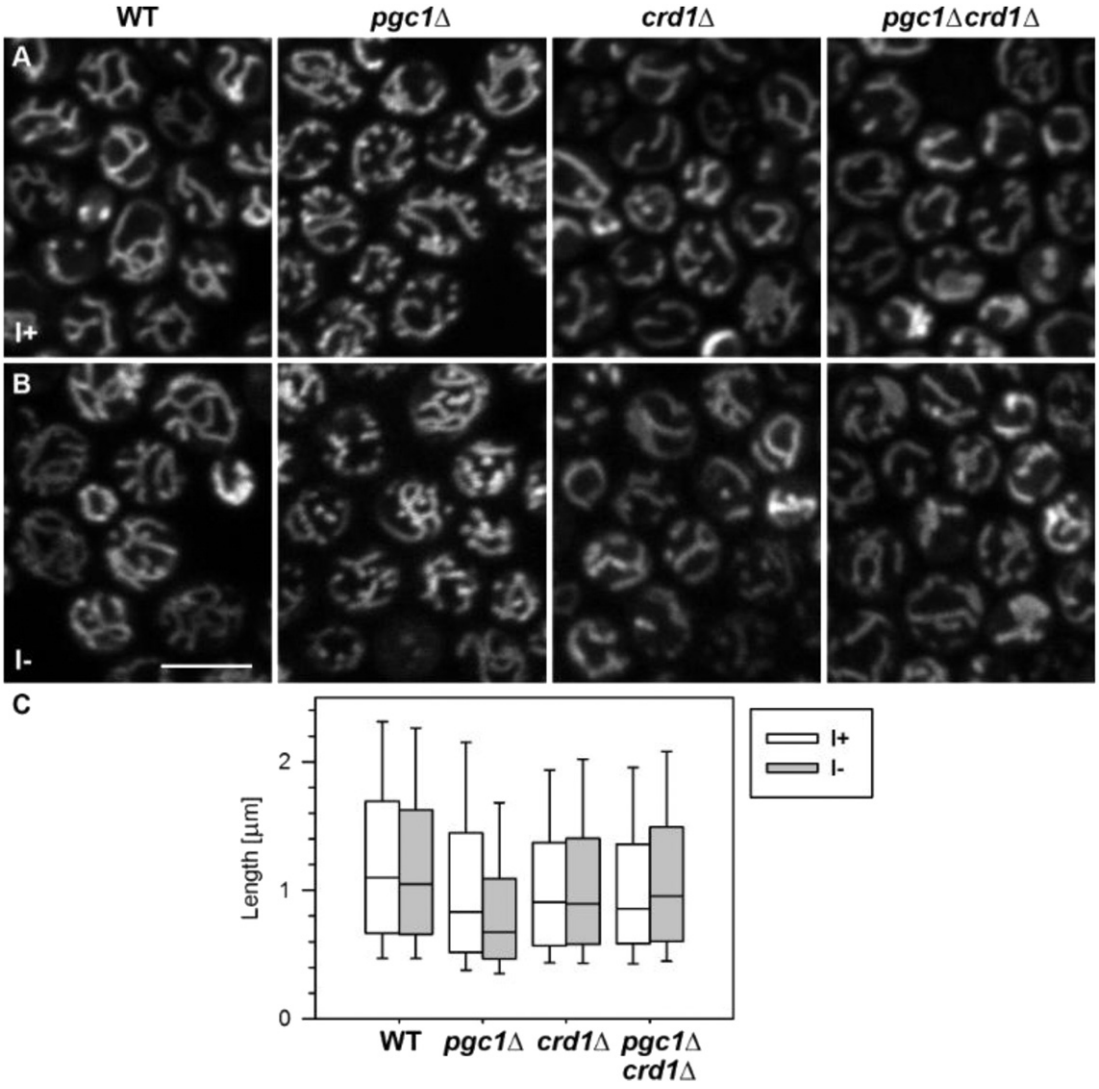

Fig. 6. Yeast cells accumulating PG exhibit fragmented mitochondria. Yeast cell were grown in SMDGE media for 24 h. A, Mitochondrial networks visualized by Mitotracker staining. Mean projections of five consecutive confocal sections with axial spacing of 370 nm encompassing the cell cortex are shown in cultures grown in presence or B, absence of inositol in the growth medium. Bar: 5 µm. C, Statistical analysis of the mitochondrial length distributions in the analyzed strains. Median (central line), first and third quartile (lower and upper box borders, respectively) and 10 and 90 percentiles (error bars) are depicted in a box plot. Data were collected in three independent experiments. At least 250 cells were analyzed in each experiment.

to mitochondrial morphology. At normal levels of CL, the accumulation of PG increases mitochondrial fragmentation while in the absence of CL, it leads to the formation of large mitochondrial sheets. Alternatively, both effects could be induced by PG reaching a certain threshold value, independent on CL content.

3.4. *pgc1Δ* cells exhibit increased respiration compared to wild type cells

To characterize the impact of excess PG on mitochondrial functions we measured the rate of O_2 consumption in mitochondria isolated from the studied strains grown in SMDGE I+ or I− media. In the presence of NADH and absence of ADP (i.e. in non-phosphorylating state) oxygen flux is mainly the result of proton leak through the IMM. Under these experimental conditions, mitochondria isolated from *pgc1Δ* yeast grown in I− media exhibited approximately two-fold higher O_2 consumption (LEAK respiration) compared to mitochondria from WT, *crd1Δ* or *pgc1Δcrd1Δ* strains (Fig. 7A). No significant difference among mitochondria isolated from cells grown in the presence of inositol was observed. Slightly higher LEAK respiration values were detected in mitochondria from *crd1Δ* and *pgc1Δcrd1Δ* yeast grown in I− compared to I+ media. Determination of the respiratory capacity of mitochondria in the ADP-activated state of OXPHOS revealed similar results: about two-fold higher OXPHOS capacity of mitochondria from *pgc1Δ* yeast grown in I− media compared to mitochondria from WT, *crd1Δ*, or *pgc1Δcrd1Δ* yeast. In I+ media, lower OXPHOS capacity was detected in *crd1Δ* and *pgc1Δcrd1Δ* mitochondria compared to mitochondria of WT and *pgc1Δ* cells (Fig. 7B). This observation was in accordance with earlier reported lower OXPHOS capacity of *crd1Δ* mutant grown in complex media [8,9,14,24,51].

Mitochondrial respiration was also analyzed in an experimentally induced uncoupled state caused by the addition of the protonophore CCCP. This allowed the measurement of the maximum electron transfer system (ETS) capacity of mitochondria. Again, the highest consumption of O_2 was detected in mitochondria from *pgc1Δ* yeast grown in I− media (Fig. 7C). Interestingly, in this strain the uncoupled respiration rates were not increased compared to the OXPHOS capacity. A similar result was observed in mitochondria from *pgc1Δ* yeast grown in I+ medium, although respiration rates were lower compared to I− media. In contrast, the respiration rates of WT mitochondria increased ~1.5-fold following artificial uncoupling by CCCP, compared to the OXPHOS respiration values, similar to previously published data [24]. These results suggest that mitochondria from *pgc1Δ* yeast are uncoupled. Mitochondria from the CL-deficient mutants exhibited significantly lower ETS capacity compared to WT mitochondria. This decrease was more

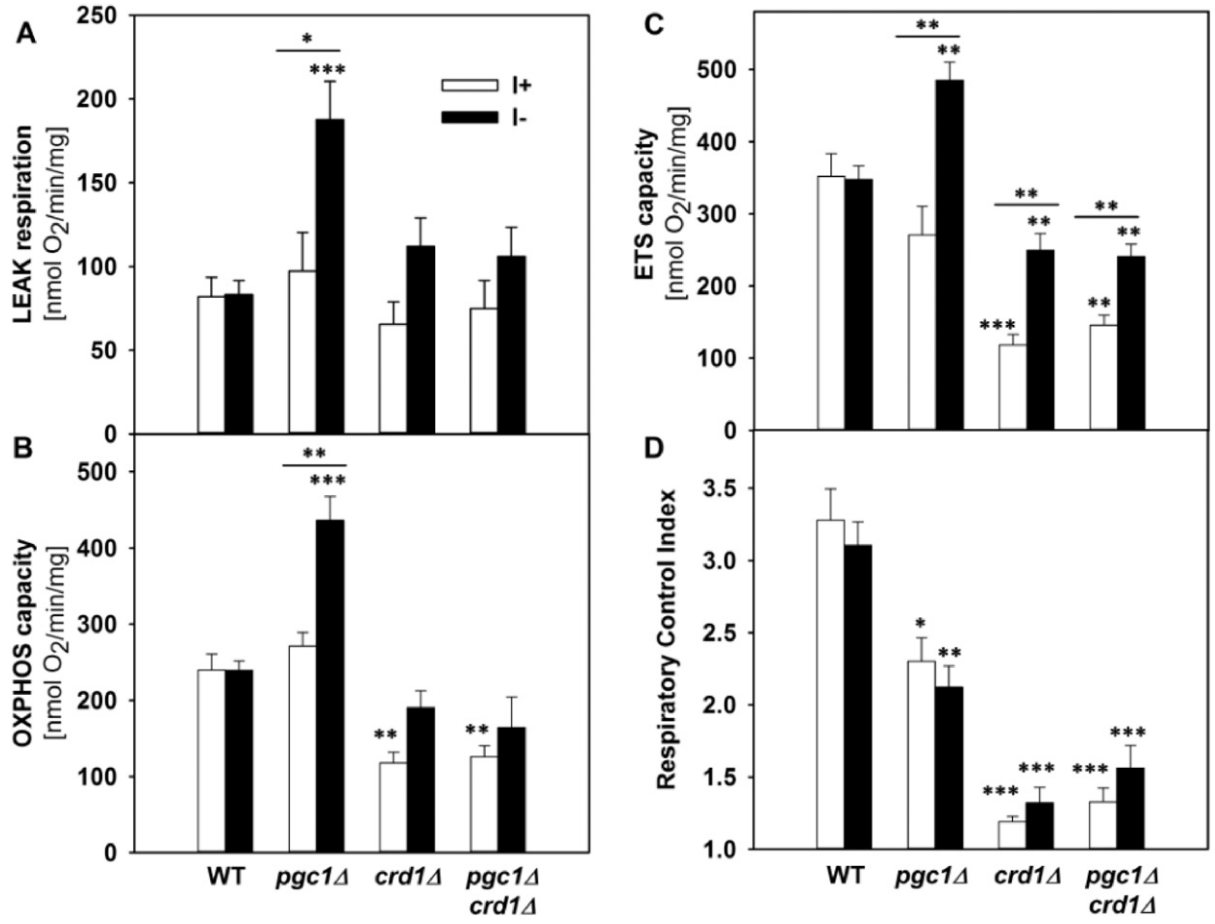

Fig. 7. Mitochondrial respiration is affected by *PGC1* deletion. Yeast cells were cultivated in SMDGE I+ or I− media for 24 h. Isolated mitochondria were used to measure of oxygen consumption. NADH was used as a respiratory substrate. Mitochondrial respiration in the presence of A, NADH (LEAK respiration); B, NADH and ADP (OXPHOS capacity) and C, protonophore CCCP (Electron Transfer System capacity). D, Respiratory control index as a measure of OXPHOS coupling. Data represent mean values of 3–6 independent experiments ± SEM. Statistically significant differences between mutant strains and WT and between I− and I+ media are marked. *, $p < 0.05$; **, $p < 0.01$; ***, $p < 0.001$.

pronounced in mitochondria isolated from *crd1Δ* and *pgc1Δcrd1Δ* yeast grown in I+ media.

Next, the respiratory control index (RCI) was calculated to measure the coupling between respiration and phosphorylation in mitochondria isolated from the mutant strains. Low RCI values detected in mitochondria isolated from *crd1Δ* and *pgc1Δcrd1Δ* cells reflected the known instability of respiratory supercomplexes induced by the absence of CL in these strains [9,11,14,24]. However, the RCI values of *pgc1Δ* mitochondria were also significantly decreased even though they contained normal levels of CL. The RCI values were insensitive to the presence of inositol in the growth medium (Fig. 7D).

3.5. PG levels modulate the activity of cytochrome c oxidase

Elevated PG has been suggested to compensate for the lack of CL in CL-deficient mitochondria [9,34]. CL is critical for the stability of the respiratory supercomplexes [14,25,26]. Therefore, we used blue native-PAGE analysis to investigate the stability of mitochondrial respiratory supercomplexes in mutants bearing the *PGC1* deletion with elevated levels of PG and standard levels of CL. Cytochrome *c* reductase (Complex III) and cytochrome *c* oxidase (Complex IV) were immunoblotted with antibodies against the subunits Rip1p and Cox2p, respectively (Fig. 8A). Complex V was visualized by "in-gel activity assay" (Fig. 8B). In agreement with previously published data [14,25,26,51,52,53], we observed a clear reduction of the amount of supercomplexes III_2IV_2 and V_2 in favor of the lower forms of supercomplexes in *crd1Δ* and *pgc1Δcrd1Δ* mutants. Interestingly, reduction of supercomplex V_2 was repeatedly less pronounced in *crd1Δ* and *pgc1Δcrd1Δ* mitochondria isolated from cells growing in the absence of inositol compared to mitochondria isolated from cells grown in the presence of inositol (Fig. 8B). The stability of respiratory supercomplexes in *pgc1Δ* cells was, however, comparable to the stability of respiratory supercomplexes of WT cells and was independent from the presence of inositol in the growth media.

Consistent with previously published data [14,53], we detected lower activity of Complex III in CL-deficient *crd1Δ* and *pgc1Δcrd1Δ* mitochondria compared to WT. In *pgc1Δ* mitochondria, activity of Complex III was also very slightly decreased (Fig. 8C). However, we observed strikingly increased activity of Complex IV in these mitochondria compared to WT. The activity of cytochrome *c* oxidase was increased 1.7-fold in mitochondria from *pgc1Δ* yeast grown in I+ media and 4.8-fold when grown in I− media (Fig. 8C). *In vitro* activity of Complex V (Fig. 8C) and in-gel activity of succinate dehydrogenase (Complex II) was also measured (data not shown), demonstrating comparable activities of these complexes in all tested strains. We conclude that excess PG in mitochondrial membranes has no influence on the stability of respiratory chain supercomplexes in mitochondria with an otherwise normal lipid composition, but induces a specific increase of Complex IV activity.

It has been shown that the absence of PG and CL resulted in translational inhibition of Cox4p, a subunit of cytochrome *c* oxidase [35]. We tested, therefore, whether an opposite situation, accumulation of PG in mitochondrial membranes of the *pgc1Δ* mutant, has any effect on Cox4p expression. We compared the relative amounts of Cox4p in mitochondria isolated from WT, *pgc1Δ*, *crd1Δ*, and *pgc1Δcrd1Δ* cells by immunoblotting (Fig. 9). No significant difference in Cox4p levels between mitochondria isolated from WT and the mutant strains were

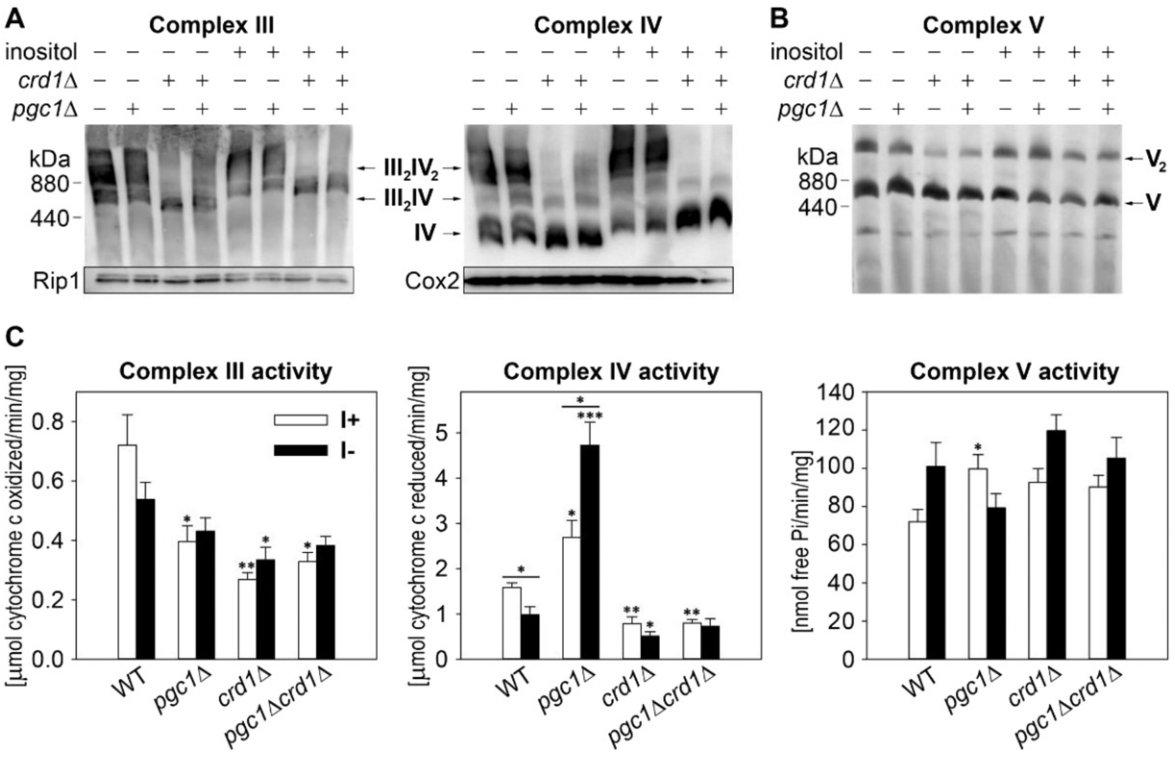

Fig. 8. Activity of Complex IV is increased in yeast strains with *PGC1* gene deletion. A, Immunoblot of mitochondrial lysates separated by blue native-PAGE using anti-Rip1p (subunit of Complex III) and anti-Cox2p (Complex IV) antibodies. Bottom panels represent immunoblots following SDS-PAGE and serve as loading controls. B, In-gel staining for Complex V activity. C, *in vitro* activities of Complex III, Complex IV and Complex V. Data in C represent mean values from 4 to 5 independent experiments ± SEM. Statistically significant differences between mutant strains and WT and between I− and I+ media are marked. *, $p < 0.05$; **, $p < 0.01$; ***, $p < 0.001$.

detected. These findings indicate that deletion of *PGC1* and the subsequent increase of PG levels has no effect on the abundance of Cox4p protein and that the observed higher activity of Complex IV is not due to increased Cox4p expression.

4. Discussion

Two routes of PG consumption in yeast have been described, *via* i) synthesis of CL by Crd1p, and ii) degradation of PG to G3P and DAG by Pgc1p. Consequently, PG accumulates in yeasts when either *CRD1* or *PGC1* is deleted [4,5,6,7,8,9]. Our data suggest that each of these deletions elevates a distinct pool of PG (Fig. 1A). Similarly, the existence of two separate PG pools was previously reported in hearts of rats after fasting or induction of diabetes [54].

In *pgc1Δ* cells the PG content decreased to WT levels upon expression of *PGC1* from a multicopy plasmid, but elevated PG levels could not be lowered in *crd1Δ* cells by overexpression of *PGC1*. In the double mutant *pgc1Δcrd1Δ*, *PGC1* overexpression reduced the PG content to the level observed in the *crd1Δ* strain (Fig. 2A). This selectivity of Pgc1p was not caused by the substrate specificity of the enzyme. It is true that we detected different fatty acid compositions of PG in the *pgc1Δ* and *crd1Δ* mutants (Fig. 2B), but at the same time, we showed that both of these pools can be consumed by Pgc1p *in vitro* (Fig. 2C). Apparently, PG dedicated for Crd1p-catalyzed CL biosynthesis is inaccessible to Pgc1p *in vivo*. We hypothesize that this limited accessibility of the Crd1p-specific PG fraction reflects a different subcellular localization of the Crd1p and Pgc1p enzymes. Crd1p activity has been localized to the matrix side of the IMM [55,56]. In the frame of the proposed model, we expect the Crd1p-specific pool of PG to localize there, too. Currently, it is not known which of the membranes hosts the Pgc1p activity. Based on our data, we suggest that the active site of Pgc1p is not exposed to the mitochondrial matrix. Additional study will be necessary to verify this hypothesis.

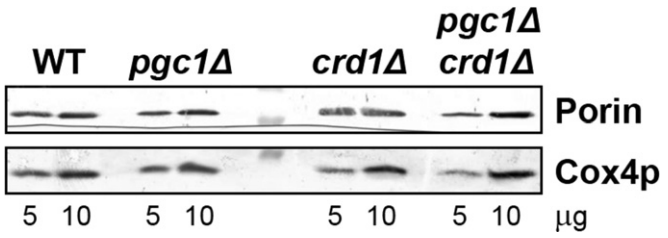

Fig. 9. The amount of Cox4p is not affected by *PGC1* deletion. Immunoblot analysis of Cox4p. Upper panel with Porin serves as a loading control. For loading, 5 (left) and 10 μg of mitochondrial protein (right) was used.

An alternative explanation of different fatty acid composition of PG in the *pgc1Δ* compared to *crd1Δ* mutant (Fig. 2B) could be raised from the interpretation that PG partially takes over some CL functions in *crd1Δ* cells [9,34]. CL is massively remodeled by the action of a phospholipase Cld1p and a transacylase Taz1p [57,58,59]. Accordingly, *cld1Δ* cells exhibit altered CL acyl composition compared to wild type. Eventual remodeling of "CL-like" PG in *crd1Δ* mutant remains hypothetical, however, as the phospholipase activity was shown to be highly CL-specific [59].

Accumulation of PG in the *PGC1* deletion strains further increased in media without inositol ([7]; Fig. 1A), where Pgs1p-catalyzed PG biosynthesis is upregulated (Fig. 3B) [42,43,45,47]. Increased accumulation of PG in I− media compared to I+ media was not observed in *crd1Δ* cells, indicating that most likely Pgc1p-mediated PG degradation compensates for increased Pgs1p activity in I− media. Importantly, expression (Fig. 3A) and *in vitro* activity of Pgc1p (not shown) was independent of inositol and *in vitro* activity of the inositol-dependent Pgs1p protein was not affected by Pgc1p expression (Fig. 3B). Higher PG accumulation in the *pgc1Δ* cells grown on the inositol-free media can be, therefore, fully ascribed to the increase in Pgs1p activity.

The role of the lipid composition in mitochondrial morphology is a well-known phenomenon [15,16,60,61,62,63,64] Results from the

analysis of mitochondrial length distribution in the *pgc1Δ* strain indicated a fragmented mitochondrial network compared to WT and CL-deficient strains (*crd1Δ* and *pgc1Δcrd1Δ*) even though the mitochondrial membranes in *pgc1Δ* cells contained normal levels of CL (Fig. 6). The occurrence of fragmented mitochondria in *pgc1Δ* cells indicates that the elevation of the Pgc1p-specific pool of PG favors mitochondrial fission over fusion, similar to the morphology found in other fusion-defective mutants [15,61,65,66,67]. In *psd1Δ* yeast, which lack the gene coding for phosphatidylserine decarboxylase crucial for the mitochondrial phosphatidylethanolamine biosynthesis, impaired mitochondrial fusion has also been described as a result of changes in the lipid composition of mitochondrial membranes [15,61].

Normal mitochondrial morphology has been reported by earlier studies in *crd1Δ* cells [15,48]. In contrast to this fact, we observed an increased occurrence of mitochondria coalesced into large, flat sheets in *crd1Δ* cells cultivated in synthetic minimal medium with a nonfermentable carbon source (Fig. 4A,B). It is known that under respiratory conditions, *crd1Δ* mutant accumulates higher amounts of PG compared to fermentative conditions [5,8]. It could be that the sheet formation is induced by higher levels of PG in *crd1Δ* cultivated in nonfermentable compared to fermentable carbon source. This holds true also for *pgc1Δcrd1Δ* cells, in which the frequency of sheets further increased with the PG content in I− media (Fig. 4C). These results suggest that formation of mitochondrial sheets could be a consequence of PG accumulation.

It is noteworthy here that the primary place for PG accumulation in strains lacking Crd1p would be the IMM. Accordingly, morphology similar to that of CL-deficient mitochondria was observed in MICOS (mitochondrial contact site and cristae organizing system) mutants defective in maintaining the IMM structure [68]. In addition, our co-localization experiments revealed a specific structure of the sheets. The mitochondrial matrix protein, Pda1p [49,50], localized exclusively to distinct foci at the border of the sheets, while the inner area of the sheet remained void of Pda1p-GFP signal, suggesting fragmentation of the IMM within these altered mitochondria.

Alterations of mitochondrial morphology often reflect changes in mitochondrial functionality and/or the energetic state of the cell [69]. Fused mitochondria are preferred when optimal mitochondrial energy production is needed or present [70,71]. In contrast, fragmented mitochondria are frequently found in resting cells and may represent a morphological state when respiration activity is damaged or not required [71,72,73]. The lack of CL in *crd1Δ* mutant was reported to cause suboptimal respiratory chain function as evidenced by decreased respiratory rates, decreased RCI, and destabilization of respiratory chain supercomplexes [8,9,14,24,25,26,34,74,75]. Based on the respiratory characteristics of the *pgc1Δ* strain, accumulation of excess PG in the presence of normal CL levels has no impact on the stability of supercomplexes III_2IV_2 and V_2 (Fig. 8A,B), and it has negligible effect on the *in vitro* activity of Complexes III and V (Fig. 8C). The major observed respiration-related impact of *PGC1* deletion was the increase in Complex IV activity. Especially in inositol-free medium, the *in vitro* activity of Complex IV was almost 5 times higher compared to the WT strain (Fig. 8C). Probably due to the aforementioned instability of the respiration supercomplexes in CL-defective strains (note the remarkable decrease of III_2IV_2 and also V_2 in cells bearing the *CRD1* gene deletion, Fig. 8A,B), this boost of Complex IV activity could not be detected in *pgc1Δcrd1Δ* cells (Fig. 8C). Accordingly, *pgc1Δ* but not *pgc1Δcrd1Δ* mitochondria exhibited an increased rate of respiration (Fig. 7 A-C), and the respiratory control index in *crd1Δ* and *pgc1Δcrd1Δ* was low compared to *pgc1Δ* strain (Fig. 7D).

It has been shown that the important factor for the supercomplex stabilization and function of Complex IV is the level of expression of Complex IV subunits [76]. Su and Dowhan reported that in the absence of anionic phospholipids, subunit of Complex IV, Cox4p, is highly repressed at the translational level [35]. Inspired by their observation, we tested whether the elevated PG in *pgc1Δ* mitochondria induced the opposite effect on Cox4p expression. The immunoblot detection revealed no difference in the amounts of this protein in the WT, *pgc1Δ*, *crd1Δ*, and *pgc1Δcrd1Δ* mitochondria, however (Fig. 9).

An alternative explanation for the increased activity of Complex IV in mitochondria with increased levels of PG is based on shape differences between cylindrical PG and conical CL molecules. In this interpretation, excess PG or rather changed ratio of PG/CL in the outer leaflet of the IMM could provoke the imbalance in the membrane curvature resulting in a leak of protons through the IMM. Complex IV in this case would be activated to maintain the electromotive force. The idea of a leaky IMM in *pgc1Δ* yeast is supported by our observation that the rate of oxygen consumption in *pgc1Δ* mitochondria following the addition of ADP (OXPHOS capacity) cannot be further increased by the addition of protonophore CCCP (Fig. 7B,C). The uncoupled respiration in the *pgc1Δ* cells corresponds well with the increased fragmentation of *pgc1Δ* mitochondria (Fig. 6). Fragmented yeast mitochondria are observed after *in vitro* dissipation of the electrical gradient across the IMM with ionophores [77], and in mammalian cells, mitochondrial fusion is strongly inhibited by treatment with protonophores [78,79].

Taken together, our results show that not only the loss of CL, but also defective removal of a direct CL precursor, PG, from the IMM significantly affects mitochondrial morphology and function. This observation strongly supports recent studies, which suggested that the decreased CL levels and/or accumulation of another CL precursor, monolysocardiolipin, could be a primary cause of mitochondrial phenotypes observed in yeast defective in CL remodeling [14,80]. It remains to be established, however, whether increased accumulation of PG *per se* contributes to observe mitochondrial defects also in mammalian cells.

Conflict of interest

None.

Supplementary data to this article can be found online at http://dx.doi.org/10.1016/j.bbabio.2015.10.004.

Acknowledgements

Supported by Scientific Grant Agency of the Ministry of Education, Science, Research and Sport of the Slovak Republic and the Slovak Academy of Sciences 1/0664/13 and 2/0168/14, the Slovak Research and Development Agency contracts No. LPP-0291-09, APVV-0123-10 and APVV-0286-12, the Czech Science Foundation 15-10641S, and NIH R01HL108882 to SMC.

We thank Jozef Ukropec (Institute of Experimental Endocrinology, Bratislava, Slovakia) for loan of the Clark-type electrode (Hansatech). We thank Ľubomír Tomáška and Peter Polčic for generous gift of antibodies and Marta Kostolanská, Petronela Melicherová and Katarína Nagyová for technical help.

References

[1] C.D. Sperka-Gottlieb, A. Hermetter, F. Paltauf, G. Daum, Lipid topology and physical properties of the outer mitochondrial membrane of the yeast, Saccharomyces cerevisiae, Biochim. Biophys. Acta 946 (1988) 227–234.
[2] R. Simbeni, L. Pon, E. Zinser, F. Paltauf, G. Daum, Mitochondrial membrane contact sites of yeast. Characterization of lipid components and possible involvement in intramitochondrial translocation of phospholipids, J. Biol. Chem. 266 (1991) 10047–10049.
[3] E. Zinser, C.D. Sperka-Gottlieb, E.V. Fasch, S.D. Kohlwein, F. Paltauf, G. Daum, Phospholipid synthesis and lipid composition of subcellular membranes in the unicellular eukaryote Saccharomyces cerevisiae, J. Bacteriol. 173 (1991) 2026–2034.
[4] F. Jiang, H.S. Rizavi, M.L. Greenberg, Cardiolipin is not essential for the growth of *Saccharomyces cerevisiae* on fermentable or non-fermentable carbon sources, Mol. Microbiol. 26 (1997) 481–491.
[5] G. Tuller, C. Hrastnik, G. Achleitner, U. Schiefthaler, F. Klein, G. Daum, YDL142c encodes cardiolipin synthase (Cls1p) and is non-essential for aerobic growth of *Saccharomyces cerevisiae*, FEBS Lett. 421 (1998) 15–18.
[6] S.C. Chang, P.N. Heacock, E. Mileykovskaya, D.R. Voelker, W. Dowhan, Isolation and characterization of the gene (CLS1) encoding cardiolipin synthase in *Saccharomyces cerevisiae*, J. Biol. Chem. 273 (1998) 14933–14941.
[7] M. Simocková, R. Holic, D. Tahotná, J. Patton-Vogt, P. Griac, Yeast Pgc1p (YPL206c) controls the amount of phosphatidylglycerol via a phospholipase C-type degradation

mechanism, J. Biol. Chem. 283 (2008) 17107–17115, http://dx.doi.org/10.1074/jbc.M800868200.
[8] Q. Zhong, V.M. Gohil, L. Ma, M.L. Greenberg, Absence of cardiolipin results in temperature sensitivity, respiratory defects, and mitochondrial DNA instability independent of pet56, J. Biol. Chem. 279 (2004) 32294–32300, http://dx.doi.org/10.1074/jbc.M403275200.
[9] F. Jiang, M.T. Ryan, M. Schlame, M. Zhao, Z. Gu, M. Klingenberg, et al., Absence of cardiolipin in the crd1 null mutant results in decreased mitochondrial membrane potential and reduced mitochondrial function, J. Biol. Chem. 275 (2000) 22387–22394, http://dx.doi.org/10.1074/jbc.M909868199.
[10] G. Paradies, V. Paradies, V. De Benedictis, F.M. Ruggiero, G. Petrosillo, Functional role of cardiolipin in mitochondrial bioenergetics, Biochim. Biophys. Acta 1837 (2014) 408–417, http://dx.doi.org/10.1016/j.bbabio.2013.10.006.
[11] E. Mileykovskaya, W. Dowhan, Cardiolipin-dependent formation of mitochondrial respiratory supercomplexes, Chem. Phys. Lipids 179 (2014) 42–48, http://dx.doi.org/10.1016/j.chemphyslip.2013.10.012.
[12] T.H. Haines, N.A. Dencher, Cardiolipin: a proton trap for oxidative phosphorylation, FEBS Lett. 528 (2002) 35–39.
[13] D. Acehan, Y. Xu, D.L. Stokes, M. Schlame, Comparison of lymphoblast mitochondria from normal subjects and patients with Barth syndrome using electron microscopic tomography, Lab. Investig, J. Tech. Methods Pathol. 87 (2007) 40–48, http://dx.doi.org/10.1038/labinvest.3700480.
[14] M.G. Baile, M. Sathappa, Y.-W. Lu, E. Pryce, K. Whited, J.M. McCaffery, et al., Unremodeled and remodeled cardiolipin are functionally indistinguishable in yeast, J. Biol. Chem. 289 (2014) 1768–1778, http://dx.doi.org/10.1074/jbc.M113.525733.
[15] A.S. Joshi, M.N. Thompson, N. Fei, M. Hüttemann, M.L. Greenberg, Cardiolipin and mitochondrial phosphatidylethanolamine have overlapping functions in mitochondrial fusion in *Saccharomyces cerevisiae*, J. Biol. Chem. 287 (2012) 17589–17597, http://dx.doi.org/10.1074/jbc.M111.330167.
[16] R.M. DeVay, L. Dominguez-Ramirez, L.L. Lackner, S. Hoppins, H. Stahlberg, J. Nunnari, Coassembly of Mgm1 isoforms requires cardiolipin and mediates mitochondrial inner membrane fusion, J. Cell Biol. 186 (2009) 793–803, http://dx.doi.org/10.1083/jcb.200906098.
[17] V.A. Patil, J.L. Fox, V.M. Gohil, D.R. Winge, M.L. Greenberg, Loss of cardiolipin leads to perturbation of mitochondrial and cellular iron homeostasis, J. Biol. Chem. 288 (2013) 1696–1705, http://dx.doi.org/10.1074/jbc.M112.428938.
[18] S.-Y. Choi, F. Gonzalvez, G.M. Jenkins, C. Slomianny, D. Chretien, D. Arnoult, et al., Cardiolipin deficiency releases cytochrome c from the inner mitochondrial membrane and accelerates stimuli-elicited apoptosis, Cell Death Differ. 14 (2007) 597–606, http://dx.doi.org/10.1038/sj.cdd.4402020.
[19] J.B. McMillin, W. Dowhan, Cardiolipin and apoptosis, Biochim. Biophys. Acta 1585 (2002) 97–107.
[20] A.S. Joshi, J. Zhou, V.M. Gohil, S. Chen, M.L. Greenberg, Cellular functions of cardiolipin in yeast, Biochim. Biophys. Acta 1793 (2009) 212–218, http://dx.doi.org/10.1016/j.bbamcr.2008.07.024.
[21] N. Sato, Roles of the acidic lipids sulfoquinovosyl diacylglycerol and phosphatidylglycerol in photosynthesis: their specificity and evolution, J. Plant Res. 117 (2004) 495–505, http://dx.doi.org/10.1007/s10265-004-0183-1.
[22] D.H. Kim, M.-J. Park, G.H. Gwon, A. Silkov, Z.-Y. Xu, E.C. Yang, et al., An ankyrin repeat domain of AKR2 drives chloroplast targeting through coincident binding of two chloroplast lipids, Dev. Cell 30 (2014) 598–609, http://dx.doi.org/10.1016/j.devcel.2014.07.026.
[23] A. Günther, C. Ruppert, R. Schmidt, P. Markart, F. Grimminger, D. Walmrath, et al., Surfactant alteration and replacement in acute respiratory distress syndrome, Respir. Res. 2 (2001) 353–364.
[24] V. Koshkin, M.L. Greenberg, Cardiolipin prevents rate-dependent uncoupling and provides osmotic stability in yeast mitochondria, Biochem. J. 364 (2002) 317–322.
[25] K. Pfeiffer, V. Gohil, R.A. Stuart, C. Hunte, U. Brandt, M.L. Greenberg, et al., Cardiolipin stabilizes respiratory chain supercomplexes, J. Biol. Chem. 278 (2003) 52873–52880, http://dx.doi.org/10.1074/jbc.M308366200.
[26] M. Zhang, E. Mileykovskaya, W. Dowhan, Gluing the respiratory chain together. Cardiolipin is required for supercomplex formation in the inner mitochondrial membrane, J. Biol. Chem. 277 (2002) 43553–43556, http://dx.doi.org/10.1074/jbc.C200551200.
[27] L.A. Luévano-Martínez, M.F. Forni, V.T. Dos Santos, N.C. Souza-Pinto, A.J. Kowaltowski, Cardiolipin is a key determinant for mtDNA stability and segregation during mitochondrial stress, Biochim. Biophys. Acta 1847 (2015) 587–598, http://dx.doi.org/10.1016/j.bbabio.2015.03.007.
[28] V. Dzugasová, M. Obernauerová, K. Horváthová, M. Vachová, M. Záková, J. Subík, Phosphatidylglycerolphosphate synthase encoded by the PEL1/PGS1 gene in *Saccharomyces cerevisiae* is localized in mitochondria and its expression is regulated by phospholipid precursors, Curr. Genet. 34 (1998) 297–302.
[29] S.C. Chang, P.N. Heacock, C.J. Clancey, W. Dowhan, The PEL1 gene (renamed PGS1) encodes the phosphatidylglycero-phosphate synthase of *Saccharomyces cerevisiae*, J. Biol. Chem. 273 (1998) 9829–9836.
[30] M. Janitor, E. Jarosch, R.J. Schweyen, J. Subík, Molecular characterization of the PEL1 gene encoding a putative phosphatidylserine synthase, Yeast 11 (1995) 1223–1231, http://dx.doi.org/10.1002/yea.320111302.
[31] Q. Zhong, J. Gvozdenovic-Jeremic, P. Webster, J. Zhou, M.L. Greenberg, Loss of function of KRE5 suppresses temperature sensitivity of mutants lacking mitochondrial anionic lipids, Mol. Biol. Cell 16 (2005) 665–675, http://dx.doi.org/10.1091/mbc.E04-09-0808.
[32] Q. Zhong, G. Li, J. Gvozdenovic-Jeremic, M.L. Greenberg, Up-regulation of the cell integrity pathway in *Saccharomyces cerevisiae* suppresses temperature sensitivity of the pgs1Delta mutant, J. Biol. Chem. 282 (2007) 15946–15953, http://dx.doi.org/10.1074/jbc.M701055200.
[33] Q. Zhong, M.L. Greenberg, Deficiency in mitochondrial anionic phospholipid synthesis impairs cell wall biogenesis, Biochem. Soc. Trans. 33 (2005) 1158–1161, http://dx.doi.org/10.1042/BST20051158.
[34] M. Zhang, X. Su, E. Mileykovskaya, A.A. Amoscato, W. Dowhan, Cardiolipin is not required to maintain mitochondrial DNA stability or cell viability for *Saccharomyces cerevisiae* grown at elevated temperatures, J. Biol. Chem. 278 (2003) 35204–35210, http://dx.doi.org/10.1074/jbc.M306729200.
[35] X. Su, W. Dowhan, Translational regulation of nuclear gene COX4 expression by mitochondrial content of phosphatidylglycerol and cardiolipin in *Saccharomyces cerevisiae*, Mol. Cell. Biol. 26 (2006) 743–753, http://dx.doi.org/10.1128/MCB.26.3.743-753.2006.
[36] S. Vaena de Avalos, X. Su, M. Zhang, Y. Okamoto, W. Dowhan, Y.A. Hannun, The phosphatidylglycerol/cardiolipin biosynthetic pathway is required for the activation of inositol phosphosphingolipid phospholipase C, Isc1p, during growth of *Saccharomyces cerevisiae*, J. Biol. Chem. 280 (2005) 7170–7177, http://dx.doi.org/10.1074/jbc.M411058200.
[37] P. Griac, M.J. Swede, S.A. Henry, The role of phosphatidylcholine biosynthesis in the regulation of the INO1 gene of yeast, J. Biol. Chem. 271 (1996) 25692–25698.
[38] M. Uemura, R.A. Joseph, P.L. Steponkus, Cold acclimation of *Arabidopsis thaliana* (effect on plasma membrane lipid composition and freeze-induced lesions), Plant Physiol. 109 (1995) 15–30, http://dx.doi.org/10.1104/pp.109.1.15.
[39] S.W. Christoperson, R.L. Glass, Preparation of milk fat methyl esters by alcoholysis in an essentially nonalcoholic solution, J. Dairy Sci. 52 (1969) 1289–1290.
[40] M.M. Bradford, A rapid and sensitive method for the quantitation of microgram quantities of protein utilizing the principle of protein-dye binding, Anal. Biochem. 72 (1976) 248–254.
[41] A. Horváth, E. Horáková, P. Dunajcíková, Z. Verner, E. Pravdová, I. Slapetová, et al., Downregulation of the nuclear-encoded subunits of the complexes III and IV disrupts their respective complexes but not complex I in procyclic *Trypanosoma brucei*, Mol. Microbiol. 58 (2005) 116–130, http://dx.doi.org/10.1111/j.1365-2958.2005.04813.x.
[42] G.M. Carman, S.A. Henry, Special issue: regulation of lipid metabolism in yeast, Biochim. Biophys. Acta 1771 (2007) 239–240, http://dx.doi.org/10.1016/j.bbalip.2006.11.001.
[43] S.A. Henry, S.D. Kohlwein, G.M. Carman, Metabolism and regulation of glycerolipids in the yeast *Saccharomyces cerevisiae*, Genetics 190 (2012) 317–349, http://dx.doi.org/10.1534/genetics.111.130286.
[44] P.M. Gaynor, S. Hubbell, A.J. Schmidt, R.A. Lina, S.A. Minskoff, M.L. Greenberg, Regulation of phosphatidylglycerolphosphate synthase in *Saccharomyces cerevisiae* by factors affecting mitochondrial development, J. Bacteriol. 173 (1991) 6124–6131.
[45] Q. Zhong, M.L. Greenberg, Regulation of phosphatidylglycerophosphate synthase by inositol in *Saccharomyces cerevisiae* is not at the level of PGS1 mRNA abundance, J. Biol. Chem. 278 (2003) 33978–33984, http://dx.doi.org/10.1074/jbc.M305242200.
[46] F. Jiang, Z. Gu, J.M. Granger, M.L. Greenberg, Cardiolipin synthase expression is essential for growth at elevated temperature and is regulated by factors affecting mitochondrial development, Mol. Microbiol. 31 (1999) 373–379.
[47] Q. He, M.L. Greenberg, Post-translational regulation of phosphatidylglycerolphosphate synthase in response to inositol, Mol. Microbiol. 53 (2004) 1243–1249, http://dx.doi.org/10.1111/j.1365-2958.2004.04202.x.
[48] S. Chen, D. Liu, R.L. Finley, M.L. Greenberg, Loss of mitochondrial DNA in the yeast cardiolipin synthase crd1 mutant leads to up-regulation of the protein kinase Swe1p that regulates the G2/M transition, J. Biol. Chem. 285 (2010) 10397–10407, http://dx.doi.org/10.1074/jbc.M110.100784.
[49] H.Y. Steensma, L. Tomaska, P. Reuven, J. Nosek, R. Brandt, Disruption of genes encoding pyruvate dehydrogenase kinases leads to retarded growth on acetate and ethanol in *Saccharomyces cerevisiae*, Yeast Chichester Engl. 25 (2008) 9–19, http://dx.doi.org/10.1002/yea.1543.
[50] Y. Cohen, Y.A. Klug, L. Dimitrov, Z. Erez, S.G. Chuartzman, D. Elinger, et al., Peroxisomes are juxtaposed to strategic sites on mitochondria, Mol. BioSyst. 10 (2014) 1742–1748, http://dx.doi.org/10.1039/c4mb00001c.
[51] S.M. Claypool, Y. Oktay, P. Boontheung, J.A. Loo, C.M. Koehler, Cardiolipin defines the interactome of the major ADP/ATP carrier protein of the mitochondrial inner membrane, J. Cell Biol. 182 (2008) 937–950, http://dx.doi.org/10.1083/jcb.200801152.
[52] M. Zhang, E. Mileykovskaya, W. Dowhan, Cardiolipin is essential for organization of complexes III and IV into a supercomplex in intact yeast mitochondria, J. Biol. Chem. 280 (2005) 29403–29408, http://dx.doi.org/10.1074/jbc.M504955200.
[53] T. Wenz, R. Hielscher, P. Hellwig, H. Schägger, S. Richers, C. Hunte, Role of phospholipids in respiratory cytochrome bc(1) complex catalysis and supercomplex formation, Biochim. Biophys. Acta 1787 (2009) 609–616, http://dx.doi.org/10.1016/j.bbabio.2009.02.012.
[54] G.M. Hatch, S.G. Cao, A. Angel, Decrease in cardiac phosphatidylglycerol in streptozotocin-induced diabetic rats does not affect cardiolipin biosynthesis: evidence for distinct pools of phosphatidylglycerol in the heart, Biochem. J. 306 (Pt 3) (1995) 759–764.
[55] M. Schlame, D. Haldar, Cardiolipin is synthesized on the matrix side of the inner membrane in rat liver mitochondria, J. Biol. Chem. 268 (1993) 74–79.
[56] M.G. Baile, Y.-W. Lu, S.M. Claypool, The topology and regulation of cardiolipin biosynthesis and remodeling in yeast, Chem. Phys. Lipids 179 (2014) 25–31, http://dx.doi.org/10.1016/j.chemphyslip.2013.10.008.
[57] Y. Xu, A. Malhotra, M. Ren, M. Schlame, The enzymatic function of tafazzin, J. Biol. Chem. 281 (2006) 39217–39224, http://dx.doi.org/10.1074/jbc.M606100200.
[58] Z. Gu, F. Valianpour, S. Chen, F.M. Vaz, G.A. Hakkaart, R.J.A. Wanders, et al., Aberrant cardiolipin metabolism in the yeast taz1 mutant: a model for Barth syndrome, Mol. Microbiol. 51 (2004) 149–158.
[59] A. Beranek, G. Rechberger, H. Knauer, H. Wolinski, S.D. Kohlwein, R. Leber, Identification of a cardiolipin-specific phospholipase encoded by the gene CLD1 (YGR110W) in yeast, J. Biol. Chem. 284 (2009) 11572–11578, http://dx.doi.org/10.1074/jbc.M805511200.

[60] C. Osman, M. Haag, C. Potting, J. Rodenfels, P.V. Dip, F.T. Wieland, et al., The genetic interactome of prohibitins: coordinated control of cardiolipin and phosphatidylethanolamine by conserved regulators in mitochondria, J. Cell Biol. 184 (2009) 583–596, http://dx.doi.org/10.1083/jcb.200810189.
[61] E.Y.L. Chan, G.A. McQuibban, Phosphatidylserine decarboxylase 1 (Psd1) promotes mitochondrial fusion by regulating the biophysical properties of the mitochondrial membrane and alternative topogenesis of mitochondrial genome maintenance protein 1 (Mgm1), J. Biol. Chem. 287 (2012) 40131–40139, http://dx.doi.org/10.1074/jbc.M112.399428.
[62] J. Rujiviphat, G. Meglei, J.L. Rubinstein, G.A. McQuibban, Phospholipid association is essential for dynamin-related protein Mgm1 to function in mitochondrial membrane fusion, J. Biol. Chem. 284 (2009) 28682–28686, http://dx.doi.org/10.1074/jbc.M109.044933.
[63] G. Meglei, G.A. McQuibban, The dynamin-related protein Mgm1p assembles into oligomers and hydrolyzes GTP to function in mitochondrial membrane fusion, Biochemistry (Mosc) 48 (2009) 1774–1784, http://dx.doi.org/10.1021/bi801723d.
[64] E.E.-J. Ha, M.A. Frohman, Regulation of mitochondrial morphology by lipids, BioFactors Oxf. Engl. 40 (2014) 419–424, http://dx.doi.org/10.1002/biof.1169.
[65] K.S. Dimmer, S. Fritz, F. Fuchs, M. Messerschmitt, N. Weinbach, W. Neupert, et al., Genetic basis of mitochondrial function and morphology in *Saccharomyces cerevisiae*, Mol. Biol. Cell 13 (2002) 847–853, http://dx.doi.org/10.1091/mbc.01-12-0588.
[66] H. Sesaki, S.M. Southard, M.P. Yaffe, R.E. Jensen, Mgm1p, a dynamin-related GTPase, is essential for fusion of the mitochondrial outer membrane, Mol. Biol. Cell 14 (2003) 2342–2356, http://dx.doi.org/10.1091/mbc.E02-12-0788.
[67] M. Zick, S. Duvezin-Caubet, A. Schäfer, F. Vogel, W. Neupert, A.S. Reichert, Distinct roles of the two isoforms of the dynamin-like GTPase Mgm1 in mitochondrial fusion, FEBS Lett. 583 (2009) 2237–2243, http://dx.doi.org/10.1016/j.febslet.2009.05.053.
[68] S. Hoppins, S.R. Collins, A. Cassidy-Stone, E. Hummel, R.M. Devay, L.L. Lackner, et al., A mitochondrial-focused genetic interaction map reveals a scaffold-like complex required for inner membrane organization in mitochondria, J. Cell Biol. 195 (2011) 323–340, http://dx.doi.org/10.1083/jcb.201107053.
[69] B. Westermann, Bioenergetic role of mitochondrial fusion and fission, Biochim. Biophys. Acta 1817 (2012) 1833–1838, http://dx.doi.org/10.1016/j.bbabio.2012.02.033.
[70] A.S. Rambold, B. Kostelecky, J. Lippincott-Schwartz, Fuse or die: shaping mitochondrial fate during starvation, Commun. Integr. Biol. 4 (2011) 752–754.
[71] M. Herlan, C. Bornhövd, K. Hell, W. Neupert, A.S. Reichert, Alternative topogenesis of Mgm1 and mitochondrial morphology depend on ATP and a functional import motor, J. Cell Biol. 165 (2004) 167–173, http://dx.doi.org/10.1083/jcb.200403022.
[72] N. Mendl, A. Occhipinti, M. Müller, P. Wild, I. Dikic, A.S. Reichert, Mitophagy in yeast is independent of mitochondrial fission and requires the stress response gene WHI2, J. Cell Sci. 124 (2011) 1339–1350, http://dx.doi.org/10.1242/jcs.076406.
[73] S. Wu, F. Zhou, Z. Zhang, D. Xing, Mitochondrial oxidative stress causes mitochondrial fragmentation via differential modulation of mitochondrial fission-fusion proteins, FEBS J. 278 (2011) 941–954, http://dx.doi.org/10.1111/j.1742-4658.2011.08010.x.
[74] V. Koshkin, M.L. Greenberg, Oxidative phosphorylation in cardiolipin-lacking yeast mitochondria, Biochem. J. 347 (Pt 3) (2000) 687–691.
[75] L. Ma, F.M. Vaz, Z. Gu, R.J.A. Wanders, M.L. Greenberg, The human TAZ gene complements mitochondrial dysfunction in the yeast taz1Delta mutant. Implications for Barth syndrome, J. Biol. Chem. 279 (2004) 44394–44399, http://dx.doi.org/10.1074/jbc.M405479200.
[76] T.-Z. Cui, A. Conte, J.L. Fox, V. Zara, D.R. Winge, Modulation of the respiratory supercomplexes in yeast: enhanced formation of cytochrome oxidase increases the stability and abundance of respiratory supercomplexes, J. Biol. Chem. 289 (2014) 6133–6141, http://dx.doi.org/10.1074/jbc.M113.523688.
[77] S. Meeusen, J.M. McCaffery, J. Nunnari, Mitochondrial fusion intermediates revealed in vitro, Science 305 (2004) 1747–1752, http://dx.doi.org/10.1126/science.1100612.
[78] F. Legros, A. Lombès, P. Frachon, M. Rojo, Mitochondrial fusion in human cells is efficient, requires the inner membrane potential, and is mediated by mitofusins, Mol. Biol. Cell 13 (2002) 4343–4354, http://dx.doi.org/10.1091/mbc.E02-06-0330.
[79] N. Ishihara, A. Jofuku, Y. Eura, K. Mihara, Regulation of mitochondrial morphology by membrane potential, and DRP1-dependent division and FZO1-dependent fusion reaction in mammalian cells, Biochem. Biophys. Res. Commun. 301 (2003) 891–898.
[80] C. Ye, W. Lou, Y. Li, I.A. Chatzispyrou, M. Hüttemann, I. Lee, et al., Deletion of the cardiolipin-specific phospholipase Cld1 rescues growth and life span defects in the tafazzin mutant: implications for Barth syndrome, J. Biol. Chem. 289 (2014) 3114–3125, http://dx.doi.org/10.1074/jbc.M113.529487.